US Army Corps
of Engineers
Hydrologic Engineering Center

A Muskingum-Cunge Channel Flow Routing Method for Drainage Networks

Technical Paper No. 135
November 1991

Papers in this series have resulted from technical activities of the Hydrologic Engineering Center. Versions of some of these have been published in technical journals or in conference proceedings. The purpose of this series is to make the information available for use in the Center's training program and for distribution within the Corps of Engineers.

The findings in this report are not to be construed as an official Department of the Army position unless so designated by other authorized documents.

The contents of this report are not to be used for advertising, publication, or promotional purposes. Citation of trade names does not constitute an official endorsement or approval of the use of such commercial products.

A Muskingum-Cunge Channel Flow Routing Method for Drainage Networks

November 1991

By

Jurgen Garbrecht
National Agricultural Water Quality Laboratory
USDA - Agricultural Research Service
Durant, OK 74702

(405) 924-5066

and

Gary W. Brunner
Hydrologic Engineering Center
U.S. Army Corps of Engineers
609 Second Street
Davis, CA 95616-4687

(916) 756-1104

TP-135

SUMMARY

A Muskingum-Cunge channel flow routing scheme is modified for application to large drainage networks with compound cross sections and for continuous long-term simulation. The modifications consist of a decoupling and separate routing of main and overbank channel flow, an introduction of a variable time step to increase model efficiency during periods of steady flow, and an internal determination of the numerical increment. The resulting hydrologic model is verified by comparing its flow routing results with those of hydraulic benchmark models solving the full unsteady flow equations. Test conditions consist of hypothetical flood hydrographs, long prismatic channels with simple and compound sections, and a third order drainage network. For the tested conditions, the model produces hydrograph peaks, times to peak and shapes that compare well with those of the hydraulic benchmarks. Hydrograph distortions due to overbank flood plain storage and multiple peaks from complex drainage networks are also well reproduced. The execution time of the model is generally one order of magnitude faster than that of the hydraulic benchmark models.

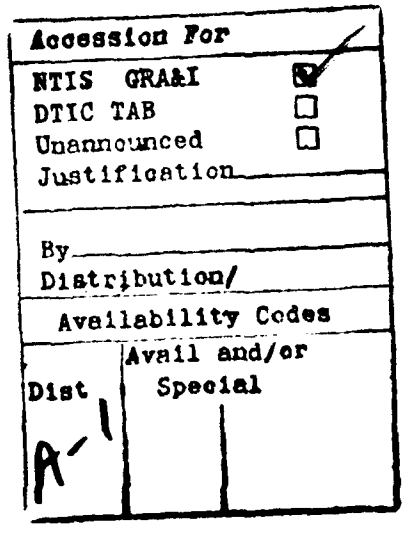

INTRODUCTION

In drainage networks, channel runoff is continuously transformed as it travels downstream. Within individual channel reaches, hydrograph characteristics change as a result of flow hydraulics, channel storage, subsurface contributions or transmission losses, and lateral inflow. In the presence of active flood plains, overbank storage produces additional attenuation. And, at channel junctions discreet changes in runoff occur as a result of the merging of flows from upstream areas. These flow transformations occur simultaneously throughout the drainage network and reshape the channel-flow hydrographs as they travel downstream. In addition to these in-channel transformations, the spatial distribution of the source areas and the timing of their respective runoff stongly influence the temporal characteristics of the watershed response. To quantify these effects in large watersheds and complex drainage networks, a practical and efficient channel flow routing model is needed. For this purpose, the Muskingum-Cunge flow routing scheme with variable parameters (Koussis, 1978; Laurenson, 1962; Ponce and Yevjevich, 1978) has been modified (Garbrecht and Brunner, 1991). The hydrologic approach greatly improves computational efficiency and speed, and reduces the amount and detail of field data traditionally needed for hydraulic routing (Weinmann and Laurenson, 1979). Such a hydrologic routing scheme is a practical approach to integrate the response from a large number of upstream source areas, to quantify effects of the flow integration processes on watershed runoff characteristics, and to investigate the impact of spatially variable source-area runoff on watershed response.

In this report, the hydrologic Drainage Network Channel Flow Routing model (DNCFR) is presented, followed by a verification for channels with simple and compound sections, and a third order drainage network. The Muskingum-Cunge flow routing scheme with variable parameters is used as the initial base model. It is adapted for separate flow routing in the main and overbank channel portions, and it includes a variable computational time increment. The parallel main and overbank channel flow routing simulates the flow characteristics in each channel portion. Differentiation between main and overbank channel flow is often desirable because sediment mobilization,

transport and deposition, transmission losses and water quality parameters vary differently in each channel portion and may require separate treatment. The variable computational time increment is introduced for efficient long-term simulation often required for sediment and water-quality investigations.

This hydrologic channel-flow routing scheme is applied to drainage networks by feeding source-area runoff into the channels, merging the channel flows at network junctions, and routing the flows through the channel network. As for most hydrologic routing schemes, the present scheme does not account for backwater effects and does not provide detailed hydraulic flow conditions along individual channel reaches nor does it reproduce localized effects. The results of the model verification show that the DNCFR is an effective tool for applications to large complex drainage networks and for continuous long-term simulations. To operate DNCFR the user must provide, in addition to the usual channel and drainage network parameters, surface and subsurface inflows into, as well as losses out of the drainage network.

MODEL DNCFR

The flow routing model DNCFR consists of four components: the first component quantifies the drainage network topology; the second the hydraulic properties of the cross sections; the third routes the flow in individual channel reaches; and the fourth is the main driver which controls the execution of individual model components and coordinates the routing within the drainage network. Each component is presented separately.

1 - Drainage Network Topology Component

In a drainage network, it is generally necessary to determine the sequence in which channel flow must be routed. When backwater effects are negligible, it is common practice to route channel flows from upstream to downstream. Such channel flow routing is called cascade routing. In drainage networks there are many upstream channels that simultaneously contribute to the watershed outlet. As a result, there are many possible sequences in which channel flows can be routed. The determination of this routing sequence is often performed manually. This is a tedious and error prone task and is least

adaptable to subsequent changes in drainage network resolution. An automated determination of the routing sequence greatly simplifies the engineer's task, insures correctness and consistency, and expedites drainage network evaluation.

One such programmable algorithm was presented by Croley (1980). His algorithm always selects the right most source node as starting point, and it determines the sequence of channel flow routing consistently from right to left on the source nodes, irrespective of drainage network configuration. Under certain conditions this approach can lead to large computer storage needs, as subsequently explained. The algorithm of model DNCFR is a direct solution algorithm (Garbrecht, 1988) based on the drainage network definition by Croley (1980). It determines a channel flow routing sequence that minimizes computer storage needs. Computer storage need is defined as the number of internal arrays required for cascade routing. An array is necessary for temporary storage of runoff results from one channel or network branch, while runoff from another is being evaluated. For example, at a junction node, runoff values from one upstream inflow must be stored, while the other upstream inflow is being evaluated. This corresponds to one storage need. Different drainage network topologies have different computer storage needs. In the following the algorithm of DNCFR to determine the routing sequence is briefly presented.

The drainage network is represented as an arrangement of channels and connecting points called nodes. The type of node is defined by the node code. A node can be a channel source, a tributary junction, a lateral inflow point, or any other special-purpose point, such as a change in channel cross section geometry or longitudinal profile node. A list of node codes that are accepted by the algorithm is given in Table 1. Between two nodes channel cross section geometry and longitudinal slope are assumed constant. It is also assumed that junctions of more than two channels at one point do not occur. However, in the remote chance of occurrence the situation can be simulated by adjacent nodes connected by a short channel. Nodes are numbered in a left hand pattern as shown in Fig. 1a and corresponding node codes are shown in Fig. 1b.

Table 1. Node code definitions.

Node Code	Definition
1	Source node
2	Drainage network outlet node
3	Channel junction node
4	Point lateral inflow node
5	Water withdrawal node
	Change in channel geometry node
	Reservoir inlet node
	Reservoir outlet node
	Water inflow node other than channel junction or point lateral flow

To determine the optimal channel flow routing sequence the Strahler channel orders (Strahler, 1956) at each node is needed. This is accomplished by having the algorithm backtrack from the source nodes downstream and increase the channel order each time a tributary of same order is encountered. When a tributary is of large Strahler order then the latter value is assumed (Fig. 1c). Once Strahler orders are assigned to all nodes, upstream and lateral inflows to each node must be identified. The algorithm identifies upstream inflows into a junction by the node numbers corresponding to the two merging channels, and lateral inflow by the node number it flows into.

With the Strahler channel order and the inflows into nodes defined, the channel flow routing sequence can easily be determined. The flow routing begins at a source node that leads to the minimum storage needs. This source node is one that directly contributes to the network order (Garbrecht, 1988). From the beginning source node, the algorithm backtracks downstream from node to node, and from network subbranch to the next larger subbranch, assigning the appropriate routing sequence to all channels, as shown in Fig. 1d. Information available upon completing the drainage network evaluation includes: 1) channel flow execution sequence, 2) identification of upstream and lateral inflows, 3) Strahler channel order at each node, 4) specification of channel or reservoir segments. This information gives a complete and sufficient description of the drainage network topology to fully automate the management of the channel flow routing process.

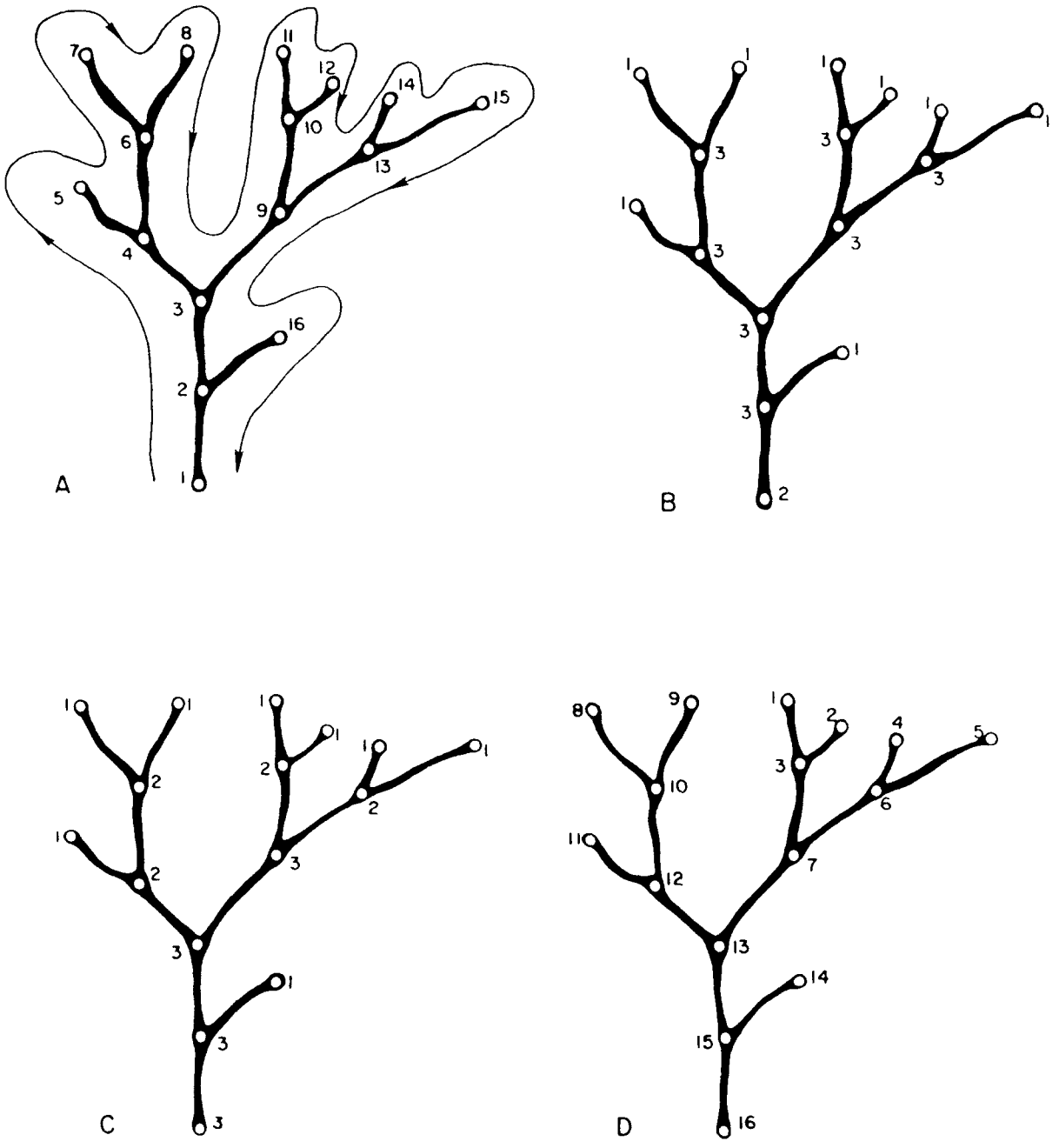

Figure 1. Schematic of a simple drainage network: a) node numbering following left hand pattern (as shown by arrow); b) node codes; c) Strahler's channel orders; d) channel flow routing sequence as determined by DNCFR.

2 - Cross Section Hydraulic Properties Component

Hydraulic properties of channel cross-sections (hereafter referred to as HPs) are required for numerical channel flow routing. HPs of interest are cross-sectional area, top width and conveyance factor. They are a function of stage, and therefore, require repeated evaluation during flow routing as stage varies with discharge. This calls for an efficient scheme to quantify the HPs. Model DNCFR uses the power function approach in which the HPs are approximated by a power function with flow depth as the independent variable (Li et al., 1975; Simons et al., 1982; Brown, 1982).

$$HP = mD^{p} \qquad (1)$$

where HP is the hydraulic property, D is flow depth and m and p are coefficients of the power function.

The coefficients of the power functions are computed by a least squared regression through the logarithm of incremental depth and HP data points. This approximation of HPs is computationally effective and generally accurate for simple concave sections. In the case of compound sections, model DNCFR performs the routing separately in the main and overbank channel portions, as previously stated and as discussed subsequently. Therefore, compound sections are broken into two simple sections, and two separate power functions, one for each channel portion, are developed as illustrated in Fig. 2 for the wetted perimeter. It is assumed that the power function accurately represents the rating curve for simple sections.

3 - Channel Flow Routing Component

The channel flow routing is based on the Muskingum-Cunge routing method with variable parameters, with further adaptations to allow for variable time and space increments, and routing in compound sections. Even though these four items are fully integrated, they are, for clarity purposes, presented separately.

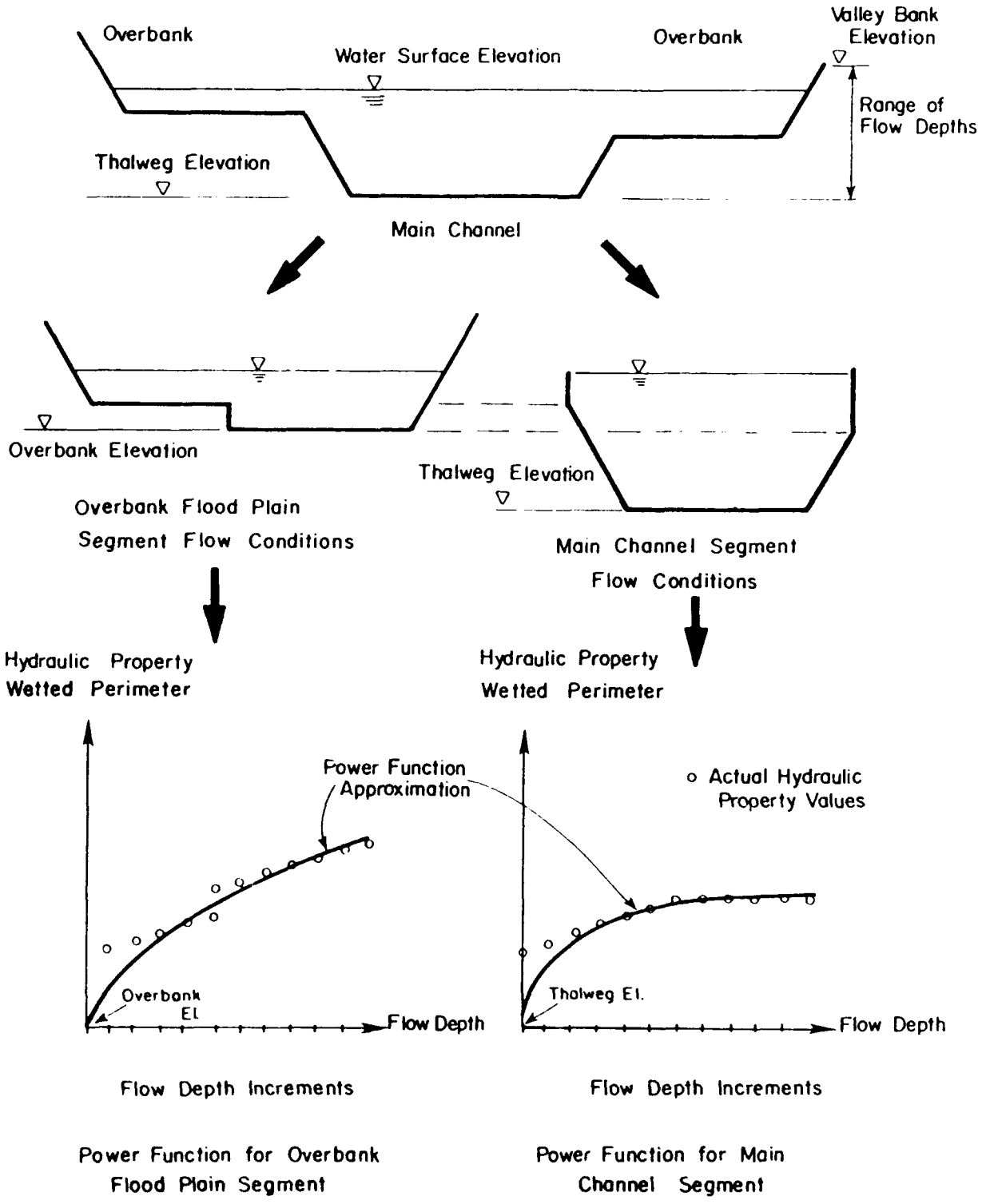

Figure 2. Schematic of wetted perimeter representation for compound cross sections (not to scale).

- Channel Flow Routing Scheme

The channel flow routing scheme is based on the Muskingum-Cunge routing method with variable parameters. The Muskingum-Cunge method, and refinements thereof, have been amply documented in previous work by Cunge (1969), Koussis (1976, 1980), Ponce (1983), Ponce and Yevjevich (1978), Smith (1980), and Weinmann and Laurenson (1979). The method is a kinematic wave routing method. The kinematic wave equation is transformed into a diffusion equation by numerical attenuation of the imperfectly centered finite-difference scheme (Smith, 1980). The method therefore accounts for hydrograph convection and diffusion, i.e. for downstream movement and peak attenuation of the hydrograph. Diffusion is introduced through two weighting coefficients which are determined from physical channel properties and flow characteristics (Cunge, 1969). When these coefficients are varied as a function of flow the method becomes a non-linear coefficient method (Koussis, 1976; Laurenson, 1962). The Muskingum-Cunge routing method with variable parameters accounts for most of the flood wave phenomena when practical applications are considered (Ponce and Theurer, 1982; Weinmann and Laurenson, 1979). The advantages of this method over other hydrologic techniques such as normal depth, Modified Puls, or simple Muskingum method are: (1) the scheme is stable with properly selected coefficients (Smith, 1980; Ponce, 1981; Ponce and Theurer, 1982); (2) it produces consistent results in that the results are reproducible with varying grid resolution (Jones, 1983; Koussis, 1983; Ponce and Theurer, 1982, 1983a and 1983b); (3) it is comparable to the diffusion wave routing (Cunge, 1969; Miller and Cunge, 1975); (4) the coefficients of the method are physically based (Cunge, 1969); (5) the method has been shown to compare well against the full unsteady flow equation over a wide range of flow situations (Ponce, 1981; Younkin and Merkel, 1988a and 1988b); and (6) the solution is largely independent of time and space intervals when these are selected within the spatial and temporal resolution criteria (Ponce, 1981; Ponce and Theurer, 1982). The essential steps of this method are briefly summarized in the following. Detailed formulations and discussions can be found in the above cited literature.

The Muskingum-Cunge routing scheme uses a storage relation to relate inflow and outflow in a channel reach. The storage relation is given by:

$$S = K[XI + (1 - X)O] \tag{2}$$

where K is a storage coefficient, X is a weighting factor, I is the inflow rate to the reach, and O is the outflow rate from the reach. The finite difference formulation of Eq. 2 results in the Muskingum Equation (Cunge, 1969; Weinmann and Laurenson, 1979):

$$Q_{j+1}^{n+1} = C_1 Q_j^n + C_2 Q_j^{n+1} + C_3 Q_{j+1}^n \tag{3}$$

with

$$C_1 = \frac{\frac{\Delta t}{K} + 2X}{F} \tag{4}$$

$$C_2 = \frac{\frac{\Delta t}{K} - 2X}{F} \tag{5}$$

$$C_3 = \frac{2(1 - X) - \frac{\Delta t}{K}}{F} \tag{6}$$

$$F = \frac{\Delta t}{K} + 2(1 - X) \tag{7}$$

where n is time superscript, j is space subscript, Q is discharge, and Δt is the routing time increment of the finite difference cell. In the original Muskingum equation, the value of the storage coefficient K and the weighting factor X are determined by trial and error or by calibration with observed hydrographs (Miller and Cunge, 1975). In the

Muskingum-Cunge approach coefficients K and X are expressed in terms of flow, channel and finite difference cell parameters (Cunge, 1969; Koussis, 1978; Ponce and Theurer, 1982; Weinmann and Lawrence, 1979) as:

$$K = \frac{\Delta x}{c} \tag{8}$$

$$X = \frac{1}{2}\left(1 - \frac{q}{S_o c \Delta x}\right) \tag{9}$$

where Δx is the space increment of the finite difference cell, c is a representative floodwave celerity, q is a representative unit width discharge, and S_o is the channel bed slope. With Eq. 8 and 9, the need of observed hydrographs to calibrate the coefficients K and X is eliminated. Cunge (1969) also demonstrated that the Muskingum-Cunge scheme, given by Eqs. 3 through 9, is equivalent to a convection-diffusion wave model, i.e. accounting for downstream movement and peak attenuation of the hydrograph.

Discharge and flood wave celerity are generally different at various points along a flood wave. To account for some of this observed nonlinearity, Koussis (1976), Weinmann and Laurenson (1980), and Ponce and Yevjevich (1978) presented the concept of variable coefficients. They redefined coefficients K and X for every computational cell as a function of updated values of unit width discharge and wave celerity. The unit width discharge and wave celerity at a grid point (j, n) are defined as:

$$c = \frac{dQ}{dA}\Big|_{j,n} \tag{10}$$

$$q = \frac{Q}{B}\Big|_{j,n} \tag{11}$$

where Q is total discharge, A is flow area, B is top width, and c is the floodwave celerity. The celerity is derived from the equation of continuity following the Kleitz-Seddon principle (Chow, 1959). The relation between discharge and flow area (Eq. 10) is based on

Manning's uniform flow equation with energy slope equal to bed slope. It is therefore a kinematic wave celerity. The average flood wave celerity for a computational cell is given as the average value of the celerity at the four nodes of the cell.

For a computational cell, the unknown unit width discharge and wave celerity are evaluated by a four-point iterative approximation (Ponce and Yevjevich, 1978). To begin the iteration an initial estimate of the discharge for the unknown grid point (j+1, n+1) is obtained using a linear projection of the known discharge at points (j, n), (j+1, n) and (j, n+1). Thereafter, a four-point iteration is used to solve for the discharge at the unknown point. The relation between discharge, flow area, top width, and flow depth is defined by power functions which are derived using cross section shape and Manning's uniform flow equation. These power functions represent simple rating curves.

The Muskingum-Cunge method with variable parameters was found to be accurate for a wide range of simple channels and flow conditions (Younkin and Merkel (1988a and 1988b)). Younkin and Merkel (1988b) performed 340 routing tests and compared the results to those from a full dynamic model used as a benchmark. They found that peak discharge, peak area, times to peak, and correlation of hydrograph shapes satisfied over 80 per cent of the Soil Conservation Service (SCS) field conditions covered by their study. The accuracy criteria used in their study were: (1) less than one percent difference for peak discharge and area; (2) one or less time step difference between time of occurrence of discharge and area peaks; and, (3) greater than ninety-five percent shape correlation for discharge and area hydrographs. However, the flow routing scheme does not account for backwater effects and it diverges from the full unsteady flow solution for very rapidly rising hydrographs in flat channels with slope less than 0.0002 (Brunner, 1989).

- Variable Computational Time Increment

Variable computational time increments are introduced to increase numerical efficiency of the routing scheme. Large time increments are used during inter-storm periods when relatively constant discharges prevail. Shorter time increments apply when discharge varies rapidly during rainfall-runoff events. The change in time increment is gradual to assure smooth transitions and to prevent a hydrograph from moving from a

region with fine computational cells to one with coarse ones.

Variable time increments are compatible with the finite difference formulation of the Muskingum-Cunge routing scheme (Eqs. 3 through 7) because the latter is an explicit scheme. Flow calculations dependent only on the current space and time increment, and they are independent of any other computational cell. As a result there are no requirements to keep Δx and Δt constant throughout the computational domain, and they may vary within limits established by the accuracy criteria set forth by Ponce and Theurer (1982).

The size of the time increment is determined as a function of rate of change in upstream inflow into the channel reach. The inflow time series is scanned ahead. If a change in discharge above a given threshold value is sensed, the current time increment is reduced; if no change in discharge is found, the size of the next time increment is increased. Upper and lower bounds for the time increment size are one day and five minutes, respectively. These boundaries were found to work well for long-term simulation in drainage networks. In addition to the smooth transition between fine and coarse time increments, the early reduction of the time increment size as an upcoming perturbation is sensed assures an adequate temporal resolution for hydrograph routing that generally satisfies the accuracy criteria of a minimum of 5 time increments on the rising portion of a hydrograph (Ponce and Theurer, 1982).

- Computational Space Increment

Computational space increments, Δx, are subreaches that define the computational cell size at which the numerical flow routing is performed. A computational space increment may be equal to the entire routing reach length or to a fraction of that length. It is initially selected as the entire reach length. If the size of this space increment does not meet the accuracy criteria for flow routing given by Ponce and Theurer (1982), it is reevaluated by subdividing the length of the routing reach into even subreaches that produce Δx's that satisfy the accuracy criteria. Ponce and Theurer's accuracy criteria is given by:

$$\Delta x \leq \frac{1}{\lambda}(\Delta x_c + \Delta x_D) \qquad (12)$$

with

$$\lambda = 2 \qquad (13a)$$

$$\Delta x_c = c\Delta t \qquad (13b)$$

$$\Delta x_D = \frac{q}{S_0} c \qquad (13c)$$

where q and c refer to a reference discharge and celerity, respectively, λ is an accuracy parameter and Δt is the minimum time increment. The minimum time increment is used because it is the one applicable during routing of a hydrograph. The reference discharge is generally two thirds of the peak flow above base flow, and the reference celerity is the celerity corresponding to the reference discharge.

The upper limit of the space increment, as given by Eq. 12, becomes quite large for very flat channels and high discharge values. In long channel reaches where such large space increments can be implemented, the flow routing may produce inaccurate hydrographs. First, the time separation between inflow and outflow hydrographs can become large resulting in the computed outflow hydrograph to end up in a region of coarse time increments. In this case the upper limit of the space increment depends on the duration and celerity of the hydrograph. Short duration and fast moving hydrographs require shorter space increments than long duration and slow moving hydrographs. As a rule of thumb the average hydrograph travel time in a space increment should not exceed about one fifth of the duration of the inflow hydrograph.

In the second case, during overbank flow conditions, long space increments may result in the hydrograph in the main channel to significantly outpace the hydrograph on the overbank portion of the cross section. This outpacing is a natural phenomena that changes hydrograph shape. Flow from main channel hydrograph spills onto the flood plains, peak runoff rate decreases, and the recession limb is stretched out as a result of

return flow from the overbanks. In the present routing scheme, the uncoupling of the main channel and overbank flow routing in very long space increments may produce an insufficient flow mixing between the two channel portions and, as a result, the effect of flood plain storage on hydrograph shape is not accurately simulated. An upper limit for the space increment of about one twentieth of the wave length was found to provide, in most cases, an adequate flow mixing. Under real world conditions tributary junctions in drainage networks and changes in cross section and flood plain characteristics generally provide short enough channel reach length that do not require limitations on the space increment.

- Routing in Compound Cross Sections

Main and overbank channel portions are separated and modeled as two independent channels. Right and left overbanks are combined into a single overbank channel. At the upstream end of a space increment total inflow discharge is divided into a main channel and an overbank flow component. Each is then routed independently using the previously described routing scheme. Momentum exchange at the flow interface between the two channel portions is neglected and the hydraulic flow characteristics are determined for each channel portion separately. At the downstream end of the space increment both flow components are summed to yield the total outflow discharge. The flow exchange between main channel and overbank channel during routing within a space increment is neglected.

Flow redistribution between main and overbank channels is based on the assumption of a constant energy head perpendicular to the flow direction and on a negligible momentum exchange at the flow interface between the two channel portions. As the stage in the main channel exceeds overbank elevation, the discharge in each channel portion is determined by matching the energy head of the flow. The energy head is computed using Bernoulli's conservation of energy equation and mean flow values for each channel portion:

$$Z_m + d_m + \frac{v_m^2}{2g} = Z_o + d_o + \frac{v_o^2}{2g} \qquad (14)$$

$$Q_T = Q_m + Q_o \qquad (15)$$

with v = Q/A; A = fct (Q, XSS, N); and d = fct (Q, XSS, N); where Z is elevation above a reference datum, v is flow velocity, XSS is channel section shape, N is channel roughness and d is flow depth. Subscript m stands for main channel, o for overbank channel, and T for total. Flow area, A, and flow depth, d, are determined as a function of cross section shape and Manning's uniform flow equation. The described separation into main and overbank flow components introduces a lateral variation in flow characteristics which make the routing scheme a quasi two dimensional approach. From the point of view of flow routing the uncoupling of main and overbank flow results in a flood wave propagation that is primarily controlled by the faster moving flow in the main channel, and a wave attenuation that is primarily controlled by the storage of the overbank channel.

4 - Coordination Component of Drainage Network Routing

This model component uses the network topology data determined in model component 1 to coordinate the routing in the drainage network. It defines and feeds the source area runoff into the channels, merges appropriate channel flows at network junctions, and executes the flow routing in proper sequence for all channel reaches. Because this model component performs simple bookkeeping tasks, no further explanations are given.

VERIFICATION APPROACH

The original Muskingum-Cunge channel flow routing with variable parameters was found to be accurate for a wide range of channel geometries and flow conditions (Koussis, 1978; Ponce, 1981; Ponce and Theurer, 1982; Younkin and Merkel, 1988a and 1988b). Brunner (1989) indicated that the method diverges from the full unsteady flow

solution for very rapidly rising hydrographs in flat channel with slopes less than 0.0002. In the context of this report, DNCFR is tested for channels with simple and compound sections and for complex drainage networks.

Verification is accomplished by comparing flow routing results with corresponding results from models solving the full unsteady flow equations. This benchmark verification approach is preferred over actual field data, because field data often includes processes unrelated to flow routing such as infiltration on overbank flood plains, or variable flow resistance due to the submergence of vegetation. These effects are generally hard to measure, and calibration to site-specific conditions is often required. The latter makes any comparison between model results and field conditions highly subjective. Benchmark verification assures well defined and identical boundary conditions. It provides an objective comparison to state-of-the-art one-dimensional hydraulic modeling capabilities.

The models selected as benchmark are DAMBRK (1988 version) of the National Weather Service (Fread, 1984) and UNET (Version 1.1) by Barkau (1990). The DAMBRK model is used for verification of flow routing in single channels with simple and compound sections. The UNET model is used to verify the flow routing in drainage networks. These models were selected because of the solution to the full dynamic flow equations and no model comparison is intended.

Verification criteria are peak discharge, time to peak, runoff volume and hydrograph shape. Discrepancies from the benchmark are quantified in percent deviation for the first three parameters. Hydrograph shape is verified visually and quantified by the correlation coefficient between computed and benchmark hydrograph values. Finally, the numerical performance of DNCFR versus the hydraulic benchmark models is defined in terms of a reduction in overall execution time.

VERIFICATION TEST CASES

Eighteen verification cases are presented. Of these, ten are single channels with simple cross sections, six are single channels with compound sections, and two are drainage networks with a mix of channels with simple and compound sections. Channel geometry, resistance to flow, and inflow hydrograph characteristics for the single channel

tests are given in Table 2. A schematic of the trapezoidal channel cross sections for test cases 2.5 and 2.6 are shown in Fig. 3. The inflow hydrographs are generated using a gamma function (Ponce and Theurer, 1982). The inflow hydrograph of test 1.4 has a dimensionless wave period, τ, greater than 171 (Table 2), and, according to Ponce at al. (1978), it is classified as a kinematic wave. Of the other inflow hydrographs seven are diffusion waves with a τ/F_r factor greater than 30, and eight are dynamic waves with a τ/F_r factor under 30. The predominance of diffusion and dynamic inflow hydrographs makes the selected hydrographs relevant for the testing of DNCFR.

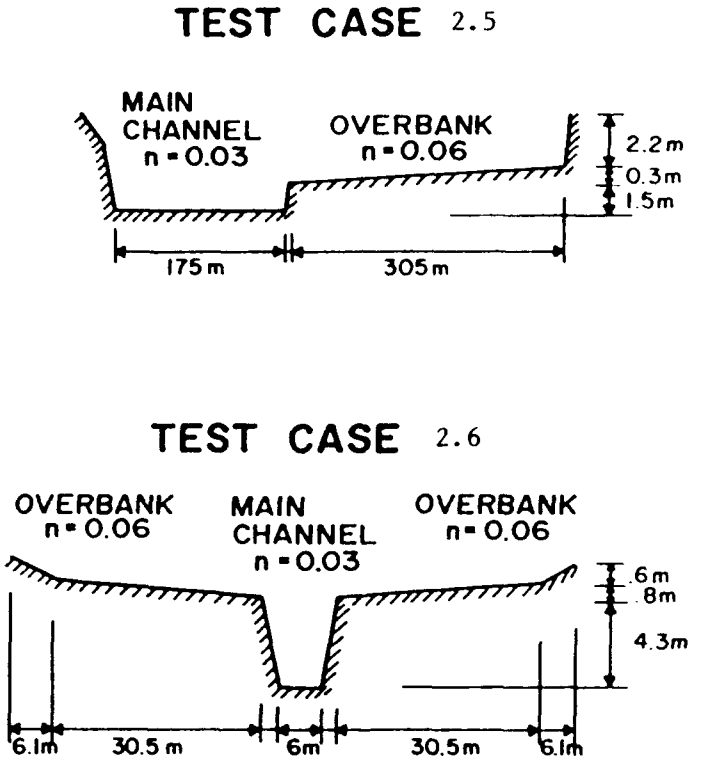

Figure 3. Schematic of cross section for test cases 2.5 and 2.6 (distorted vertical scale).

The hypothetical drainage network for the two network tests are shown in Fig. 4. The watershed is approximately 17 km long and 9 km wide. Channel slopes vary from 0.0016 to 0.004; first and second order channels have no overbank flood plains; third order channels have significant flood plains. The inflow hydrographs are mostly of the

Table 2: Channel geometry and inflow hydrograph characteristics.

Test number	CHANNEL Length	Slope	Shape	Top width Main	Top width O.B.	Depth Main	Depth O.B.	Manning's n Main	Manning's n O.B.	HYDROGRAPH Peak discharge	Base flow	Time to peak	τ	τ/F_r
	km	-	-	m	m	m	m	-	-	cms	cms	min		
1.1	25.	.002	Rect	300.0	NA	10.0	NA	.04	NA	2000	1000	60	13	32
1.2	25.	.002	Rect	300.0	NA	10.0	NA	.04	NA	2000	1000	180	39	94
1.3	25.	.008	Rect	300.0	NA	10.0	NA	.04	NA	2000	1000	60	119	154
1.4	25.	.008	Rect	300.0	NA	10.0	NA	.04	NA	2000	1000	180	357	463
1.5	25.	.0006	Rect	300.0	NA	10.0	NA	.04	NA	2000	1000	60	2	8.5
1.6	25.	.0006	Rect	300.0	NA	10.0	NA	.04	NA	2000	1000	180	5.7	24
1.7	25.	.0002	Rect	300.0	NA	10.0	NA	.04	NA	2000	1000	60	0.3	2.4
1.8	25.	.0002	Rect	300.0	NA	10.0	NA	.04	NA	2000	1000	180	1	7
1.9	29.	.00038	Rect	175.0	NA	5.0	NA	.03	NA	1250	170	370	8	31
1.10	29.	.00028	Rect	175.0	NA	5.0	NA	.03	NA	1270	170	370	3	18
2.1	25.	.002	Rect	100.0	400.0	3.8	5.0	.04	0.6	2000	300	60	12	29
2.2	25.	.002	Rect	100.0	400.0	3.8	5.0	.04	0.6	2000	300	180	32	75
2.3	25.	.0006	Rect	100.0	400.0	3.8	5.0	.04	0.6	2000	300	60	1.9	8.3
2.4	25.	.0006	Rect	100.0	400.0	3.8	5.0	.04	0.6	2000	300	180	1.7	6.9
2.5	29.	.002	Trap	178.0	305.0	1.5	2.5	.03	0.6	1256	170	360	60	158
2.6	29.	.0019	Trap	9.0	73.2	4.3	1.0	.03	0.6	211	2.8	360	54	132

τ = Dimensionless wave period; F_r = Froud Number.
O.B. = Overbank flood plains; NA = Not applicable.

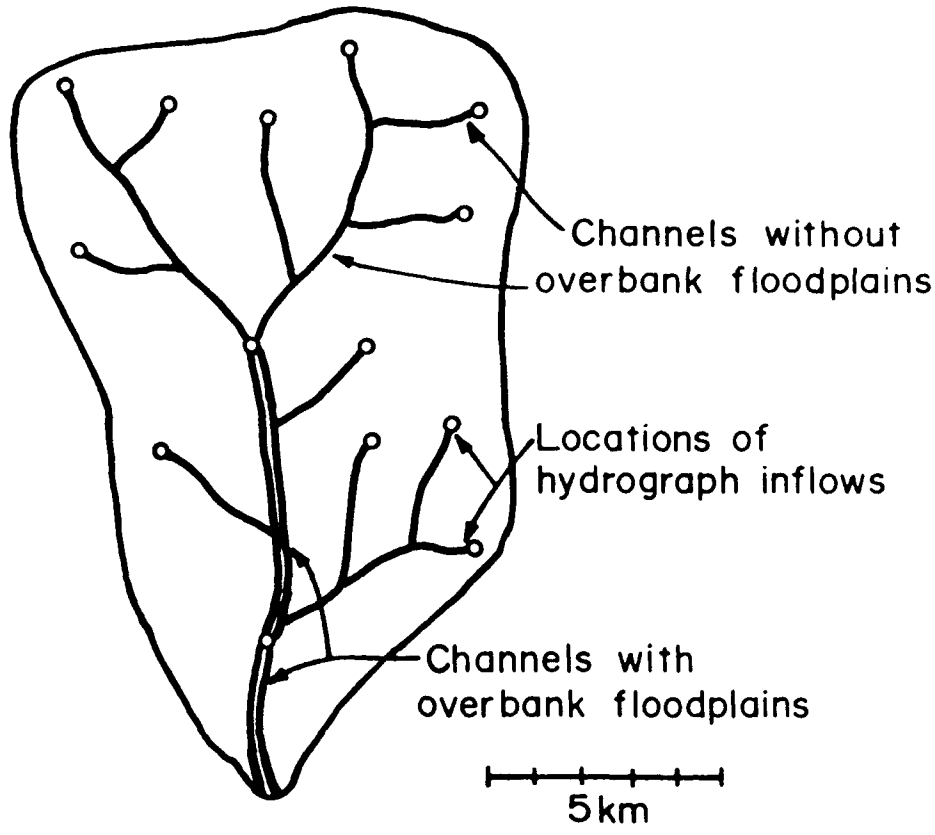

Figure 4. Hypothetical drainage network for tests 3.1 and 3.2.

diffusion type, and are entered at source nodes and selected junction nodes as indicated by hollow circles in Fig. 4. Peak and time to peak of the inflow hydrograph are chosen arbitrarily; they range from 3.0 to 7.5 cms, and 55 to 80 min, respectively, for test 3.1; and from 3.0 to 6.5 cms and 145 to 170 min, respectively, for test 3.2. Hydrograph shapes are generated using a gamma function. A storm movement at about 20 km/hr is assumed from the outlet to the top of the basin.

RESULTS OF VERIFICATION

The results of the verification are shown in Table 3. For channels with simple sections, hydrograph peak and time to peak are, on the average, less than 3% off the

Table 3: Verification results of benchmark and DNCFR, and differences between the two.

	BENCHMARK				DNCFR				DIFFERENCE			
Test	Peak discharge Q cms	Time to peak T_p min	Volume V $10^7 m^3$	Execution time* T_e sec	Peak discharge Q cms	Time to peak T_p min	Volume V $10^7 m^3$	Execution time* T_e sec	ΔQ %	ΔT_p %	ΔT_e %	Shape Correlation *100
1.1	1643.1	186	8.94	ND	1654.0	185	8.94	6	0.7	-0.5	NA	100
1.2	1916.2	300	9.55	ND	1921.4	300	9.55	6	0.3	0.0	NA	100
1.3	1916.5	138	8.94	ND	1968.2	135	8.95	4	2.7	-2.2	NA	100
1.4	1978.5	252	9.55	136	1984.5	255	9.55	6	0.3	1.2	-96	100
1.5	1309.0	226	8.94	ND	1275.3	235	8.94	4	-2.6	4.0	NA	99
1.6	1670.4	348	9.55	ND	1642.2	360	9.55	5	-1.7	3.5	NA	100
1.7	1176.0	210	8.94	74	1120.6	205	8.94	3	-4.8	2.4	-96	94
1.8	1433.9	348	9.55	ND	1337.1	355	9.55	3	-6.7	2.0	NA	97
1.9	1136.1	570	5.65	ND	1108.4	585	5.65	3	-2.4	2.6	NA	100
1.10	1079.4	585	5.65	ND	1024.5	615	5.65	3	-5.1	5.1	NA	100
						Av. of abs. values			2.7	2.3	-96	99
2.1	1058.6	216	3.11	1050	980.1	214	3.11	14	-7.4	-0.9	-99	96
2.2	1588.6	420	4.14	1656	1598.6	425	4.14	22	0.6	1.2	-99	95
2.3	605.5	396	3.11	ND	586.6	425	3.11	18	-3.1	7.3	NA	98
2.4	1017.6	525	4.14	ND	1095.5	544	4.14	18	7.7	3.6	NA	98
2.5	1238.3	605	4.17	396	1210.6	604	4.16	46	-2.2	-0.2	-88	97
2.6	193.9	665	0.6	294	198.1	675	0.58	46	2.2	1.5	-84	98
						Av. of abs. values			3.9	2.5	-93	97
3.1	47.0	325	0.092	623	49.8	315	0.091	56	6.0	-3.0	-83	97
3.2	68.7	370	0.143	985	76.8	364	0.149	62	11.8	-1.7	-94	100
						Av. of abs. values			8.9	2.3	-89	98

* Duration of simulation: 24 hrs; minimum time increments: 5 min.; includes I/O.
ND: No data; NA: not applicable.

benchmark values; for compound sections they are, on the average, less than 4% off the benchmark values. In general, tests having hydrographs of the dynamic type (tests 1.5, 1.6, 1.7, 1.8, 2.1, 2.3, and 2.4) display a larger discrepancy than those having hydrographs of the diffusion type (tests 1.1, 1.2, 1.3, 2.2, 2.5, and 2.6). This is to be expected because DNCFR is equivalent to a diffusion routing method (Cunge, 1969), and it does not account for dynamic effects. Considering the highly dynamic character of some of the hydrographs, the results of DNCFR are good for a hydrologic routing method. For example, in channels with simple sections and dynamic hydrographs (tests 1.5, 1.6, 1.7, and 1.8), about 91% of the attenuation is reproduced by DNCFR. For channels with compound sections, about 94% of the total attenuation (due to diffusion and storage) is reproduced by DNCFR.

Figure 5 show a plot of discharge and time to peak from DNCFR versus corresponding benchmark values. The data represents all tests of Table 1, including the two network applications. Neither discharge nor the time to peak show significant deviations from the line of perfect agreement. In the following peak discharge, time to peak and hydrograph shape are discussed in more detail for selected tests.

With respect to the drainage network tests, the complex hydrographs are the result of the drainage network configuration and movement of the storm up the watershed. The runoff from the lower right network branch arrives first at the outlet followed by the main peak from the upper portion of the watershed. The higher peak values by DNCFR are primarily the result of limitations regarding backwater and reverse flow effects. Indeed, the hydraulic simulations include reverse flow up tributary branches. Reverse flow is the result of high stages in the main channel while low stages prevail on the tributaries. The net effect of this reverse flow is additional storage and attenuation of the peak. Times to peak and hydrograph shapes are well reproduced for both network applications. The hydrographs leaving the drainage network are shown in Fig. 6. Peak, timing and shapes are well reproduced. The correlation coefficient for hydrograph shape is 0.98.

For simple and compound sections, the average correlation coefficient for hydrograph shape is 0.99 and 0.97, respectively. Test 1.6 is a dynamic wave with a 35% attenuation of the peak above base flow. In this case, like in all other dynamic cases, the

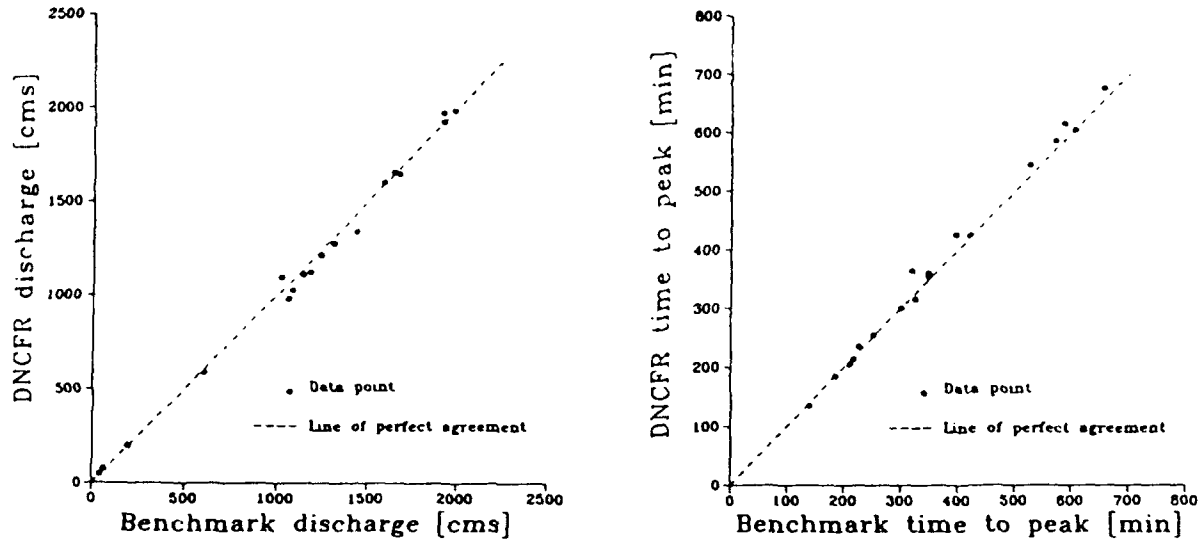

Figure 5. Benchmark vs. computed discharge and time to peak; all verification test results.

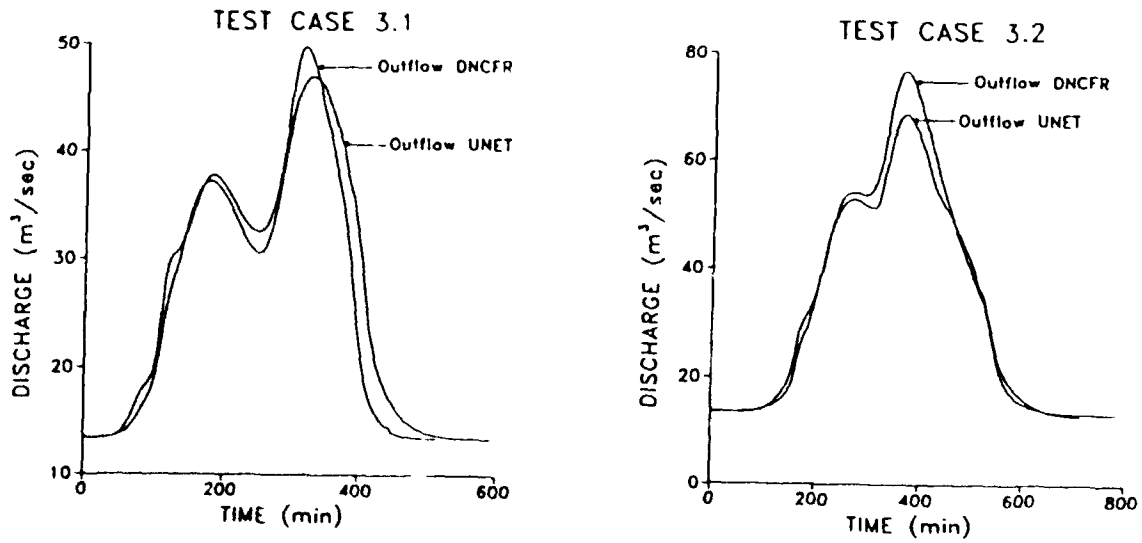

Figure 6. Hydrographs for tests 3.1 and 3.2.

hydrograph computed by DNCFR displays a larger attenuation than the benchmark. As a result of the lower flow, the time to peak lags slightly behind the benchmark value. Test 1.9 is a diffusion wave with 11% attenuation of the peak above base flow. It is typical of most diffusion wave cases with little discrepancy in peak, time to peak and hydrograph shape.

Outflow hydrographs for channels with compound section are given by tests 2.1, 2.2, 2.5 and 2.6 which are shown in Fig. 7. Test 2.1 shows a hydrograph that is attenuated entirely below overbank flood plain elevation. This example also shows the effect of the slower moving overbank flow by producing a longer hydrograph recession limb. In the other three test cases, overbank flow is active along the entire channel length. For these cases the location of beginning of overbank flow is clearly defined by the breaks in the rising limb of the hydrographs. Overall, the distortions of hydrograph shape due to overbank flood plains are consistent with the benchmark shapes.

Finally, the execution time of DNCFR is, on the average, 92% shorter than for the benchmark hydraulic evaluation (Table 3). The comparison is made on an IBM compatible PC, having an 80836 - 20MHZ micro-processor and math co-processor, and using the Microsoft FORTRAN compiler Version 5.0 with optimization. Program I/O and support computations are included in the execution time. Using the average execution time over all tests, the reduction is from 10 minutes to 32 seconds, which is a factor of 20, or about 1.2 orders of magnitude. It is believed that additional reductions in execution time can be achieved for long-term simulations because significantly larger time increments are used by the model for nearly constant discharge values that generally prevail between storm events.

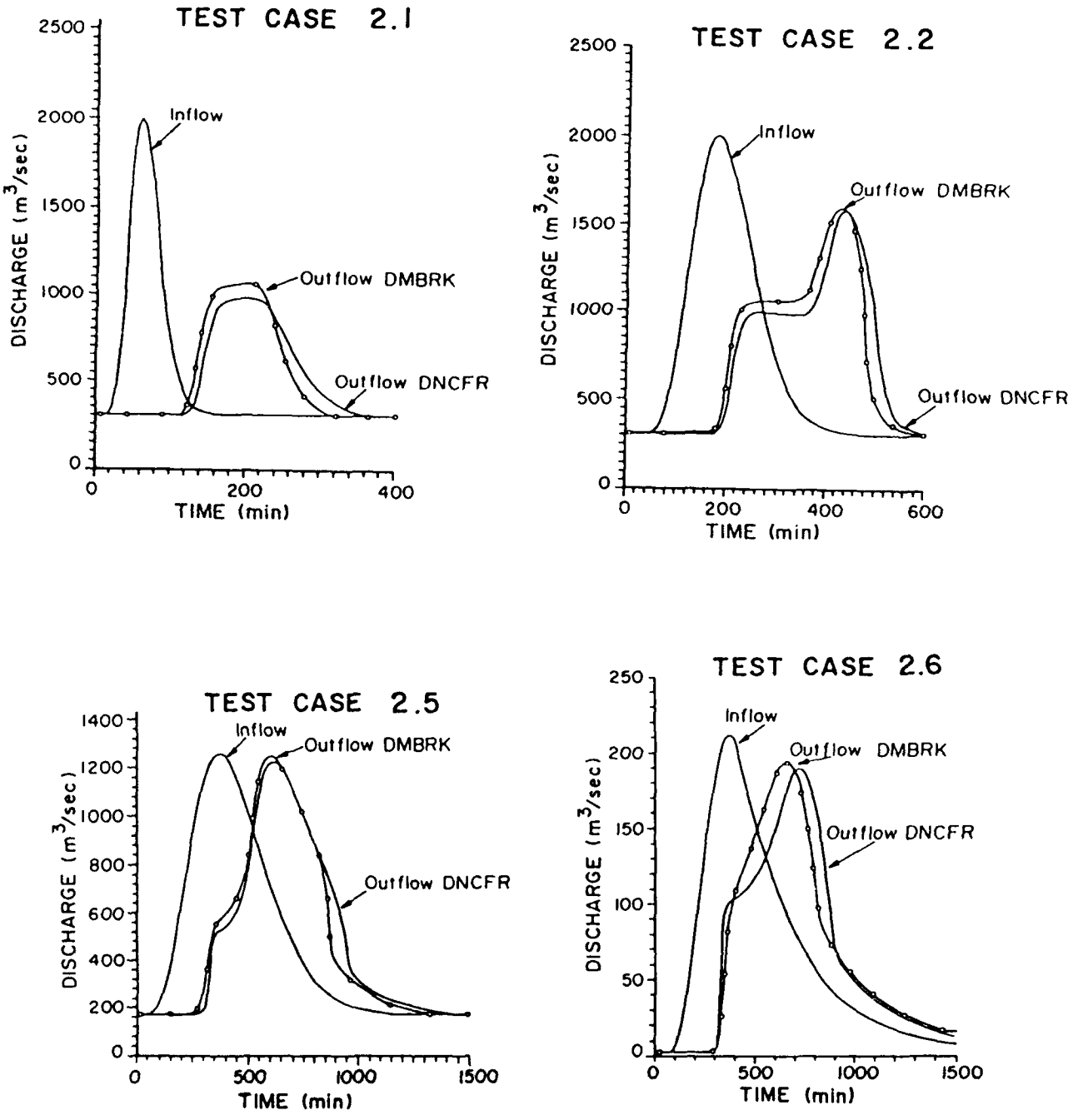

Figure 7. Verification hydrographs for tests 2.1, 2.2, 2.5, and 2.6.

SUMMARY AND CONCLUSIONS

The Muskingum-Cunge channel flow routing scheme with variable parameters is modified to account for compound sections, to include a variable time step, and to determine internally the computational reach increment. The resulting model, DNCFR, is verified for hypothetical channel and flow conditions. Routing results are compared with those of hydraulic models solving the full unsteady flow equations. Ten channels with simple sections, six with compound sections and two drainage network applications are selected for verification. For all tested cases, DNCFR reproduces the peak, time to peak and shape of the benchmark hydrograph with reasonable accuracy. Slight discrepancies (less than 10%) in the drainage network application are due to the limitations of hydrologic models with respect to backwater and reverse flow effects. The size of the discrepancy is well within the usual error of drainage network parameterization and lateral channel inflow determination. Program efficiency, as measured by the reduction in execution time, is, on the average, one order of magnitude faster than the benchmark hydraulic routing. The results of the verification indicate DNCFR to be an effective tool for hydrologic routing applications to large complex drainage networks and for continuous long-term simulations.

REFERENCES

1. Barkau, R. L. 1990. UNET One-dimensional Unsteady Flow Through a Full Network of Open Channels. User Manual, Version 1.1, St. Louis, MO.
2. Brown, G. O. 1982. Known Discharge Uncoupled Sediment Routing. Ph.D. Thesis, Colorado State University, Fort Collins.
3. Brunner, G. 1989. Muskingum-Cunge Channel Routing. Lecture Notes. HEC, U.S. Army Corps of Engineer, Davis, CA.
4. Chow, V. T. 1959. Open Channel Hydraulics. McGraw-Hill, New York.
5. Croley, T. E. 1980. A Micro-Hydrology Computation Ordering Algorithm, J. of Hyd. 48:221-236.
6. Cunge, J. A. 1969. On the Subject of a Flood Propagation Computation Method (Muskingum Method). J. of Hydraulic Res., 7(2):205-230.
7. Fread, D. L. 1984. DAMBRK: The NWS Dam-Break Flood Forecasting Model. Office of Hydrology, NWS, Nat. Oc. and Atm. Adm., U.S. Dept. of Commerce, Silver Spring, MD.
8. Garbrecht, J. 1988. Determination of the Execution Sequence of Channels in a Drainage Network for Cascade Routing. Hydrosoft, Computational Mechanics Publ., 1:129-138.
9. Garbrecht, J., and Brunner, G. 1991. Hydrologic Channel Flow Routing for Drainage Networks. J. of Hydraulics Div., ASCE, 117(5):629-642.
10. Jones, S. B. 1983. Discussion of "Accuracy Criteria in Diffusion Routing." J. of Hydr. Div., ASCE, 109(5):801-803.
11. Koussis, A. D. 1976. An Approximate Dynamic Flood Routing Method. Proc. of Int. Symp. on Unsteady Flow in Open Channels, Paper L1, Newcastle-Upon-Tyne, UK.
12. Koussis, A. D. 1980. Comparison of Muskingum Method Difference Schemes. J. of Hydr. Div., ASCE, 106(5):925-929.
13. Kousis, A. D. 1983. Discussion of "Accuracy Criteria in Diffusion Routing." J. of Hydr. Div., ASCE, 109(5):803-806.

14. Koussis, A. D. 1978. Theoretical Estimations of Flood Routing Parameters. J. of Hydraulic Div., ASCE, 104(HY1):109-115.

15. Laurenson, E. M. 1962. Hydrograph Synthesis by Runoff Routing. Report No. 66, Water Research Lab., University of South Wales, UK.

16. Li, R. M., Simons, D. B., and Sterns, M. A. 1975. Nonlinear Kinematic Wave Approximation for Water Routing. Water Resour. Res. II (2):245-252.

17. Miller, W. A., and Cunge, J. A. 1975. Simplified Equations of Unsteady Flow. "Unsteady Flow in Open Channels. K. Mahmood and V. Yevjevich, eds., Water Resour. Pub., Ft. Collins, CO.

18. Ponce, V. M. 1981. Development of an Algorithm for the Linearized Diffusion Method of Flood Routing. SDSU, Civil Engin. Series No. 81144, San Diego State University, San Diego, CA.

19. Ponce, V. M. 1983. Development of Physically Based Coefficients for the Diffusion Method of Flood Routing. Contract No. 53-3A75-3-3, U.S. Soil Conservation Service, Lanham, Maryland, U.S.

20. Ponce, V. M. and F. D. Theurer. 1982. Accuracy Criteria in Diffusion Routing. J. of Hydraulics Div., ASCE, 108(HY6):747-757.

21. Ponce, V. M., and Theurer, F. D. 1983a. Closure to "Accuracy Criteria in Diffusion Routing." J. Hydr. Div., ASCE, 109(5):806-807.

22. Ponce, V. M., and Theurer, F. D. 1983b. Closure to "Accuracy Criteria in Diffusion." J. Hydr. Div., ASCE, 109(10), 1397.

23. Ponce, V. M., R. M. Li, and D. B. Simons. 1978. Applicability of Kinematic and Diffusion Models. J. of Hydraulics Div., ASCE, 104(HY3):353-360.

24. Ponce, V. M. and V. Yevjevich. 1978. Muskingum Cunge Method with Variable Parameters. J. of Hydraulics Div., ASCE, 104(HY12):1663-1667.

25. Simons, Li and Associates. 1982. Engineering Analysis of Fluvial Systems. Simons, Li and Assoc., Fort Collins, CO.

26. Smith, A. A. 1980. A Generalized Approach to Kinematic Flood Routing. J. of Hydrology, 45:71-89.

27. Strahler, A. N. 1956. Quantitative Analysis of Watershed Geomorphology, Trans. of Am. Geoph. Union, 38(6):913-920.

28. Weinmann, P. E., and E. M. Laurenson. 1979. Approximate Flood Routing Methods: A Review. J. of Hydraulic Div., ASCE 105(HY2):1521-1535.

29. Younkin, L. M., and W. H. Merkel. 1988a. Range of Application for Reach Routing with the Variable Parameter Diffusion Model. 24th Annual Am. Water Resources Assoc. Conf., Milwaukee, WI.

30. Younkin, L. M., and W. H. Merkel. 1988b. Evaluation of Diffusion Models for Flood Routing. In Proc. of Nat. Conf. on Hydraulic Eng., ASCE, Colorado Springs, CO, :674-680.

TECHNICAL PAPER SERIES
($2 per paper)

TP-1 Use of Interrelated Records to Simulate Streamflow
TP-2 Optimization Techniques for Hydrologic Engineering
TP-3 Methods of Determination of Safe Yield and Compensation Water from Storage Reservoirs
TP-4 Functional Evaluation of a Water Resources System
TP-5 Streamflow Synthesis for Ungaged Rivers
TP-6 Simulation of Daily Streamflow
TP-7 Pilot Study for Storage Requirements for Low Flow Augmentation
TP-8 Worth of Streamflow Data for Project Design - A Pilot Study
TP-9 Economic Evaluation of Reservoir System Accomplishments
TP-10 Hydrologic Simulation in Water-Yield Analysis
TP-11 Survey of Programs for Water Surface Profiles
TP-12 Hypothetical Flood Computation for a Stream System
TP-13 Maximum Utilization of Scarce Data in Hydrologic Design
TP-14 Techniques for Evaluating Long-Term Reservoir Yields
TP-15 Hydrostatistics - Principles of Application
TP-16 A Hydrologic Water Resource System Modeling Techniques
TP-17 Hydrologic Engineering Techniques for Regional Water Resources Planning
TP-18 Estimating Monthly Streamflows Within a Region
TP-19 Suspended Sediment Discharge in Streams
TP-20 Computer Determination of Flow Through Bridges
TP-21 An Approach to Reservoir Temperature Analysis
TP-22 A Finite Difference Method for Analyzing Liquid Flow in Variably Saturated Porous Media
TP-23 Uses of Simulation in River Basin Planning
TP-24 Hydroelectric Power Analysis in Reservoir Systems
TP-25 Status of Water Resource Systems Analysis
TP-26 System Relationships for Panama Canal Water Supply
TP-27 System Analysis of the Panama Canal Water Supply
TP-28 Digital Simulation of an Existing Water Resources System
TP-29 Computer Applications in Continuing Education
TP-30 Drought Severity and Water Supply Dependability
TP-31 Development of System Operation Rules for an Existing System by Simulation
TP-32 Alternative Approaches to Water Resource System Simulation
TP-33 System Simulation for Integrated Use of Hydroelectric and Thermal Power Generation
TP-34 Optimizing Flood Control Allocation for a Multipurpose Reservoir
TP-35 Computer Models for Rainfall-Runoff and River Hydraulic Analysis
TP-36 Evaluation of Drought Effects at Lake Atitlan
TP-37 Downstream Effects of the Levee Overtopping at Wilkes-Barre, PA, During Tropical Storm Agnes
TP-38 Water Quality Evaluation of Aquatic Systems
TP-39 A Method for Analyzing Effects of Dam Failures in Design Studies
TP-40 Storm Drainage and Urban Region Flood Control Planning
TP-41 HEC-5C, A Simulation Model for System Formulation and Evaluation
TP-42 Optimal Sizing of Urban Flood Control Systems
TP-43 Hydrologic and Economic Simulation of Flood Control Aspects of Water Resources Systems
TP-44 Sizing Flood Control Reservoir Systems by Systemsm Analysis
TP-45 Techniques for Real-Time Operation of Flood Control Reservoirs in the Merrimack River Basin
TP-46 Spatial Data Analysis of Nonstructural Measures
TP-47 Comprehensive Flood Plain Studies Using Spatial Data Management Techniques
TP-48 Direct Runoff Hydrograph Parameters Versus Urbanization
TP-49 Experience of HEC in Disseminating Information on Hydrological Models
TP-50 Effects of Dam Removal: An Approach to Sedimentation
TP-51 Design of Flood Control Improvements by Systems Analysis: A Case Study
TP-52 Potential Use of Digital Computer Ground Water Models
TP-53 Development of Generalized Free Surface Flow Models Using Finite Element Techniques
TP-54 Adjustment of Peak Discharge Rates for Urbanization
TP-55 The Development and Servicing of Spatial Data Management Techniques in the Corps of Engineers
TP-56 Experiences of the Hydrologic Engineering Center in Maintaining Widely Used Hydrologic and Water Resource Computer Models
TP-57 Flood Damage Assessments Using Spatial Data Management Techniques
TP-58 A Model for Evaluating Runoff-Quality in Metropolitan Master Planning
TP-59 Testing of Several Runoff Models on an Urban Watershed
TP-60 Operational Simulation of a Reservoir System with Pumped Storage
TP-61 Technical Factors in Small Hydropower Planning
TP-62 Flood Hydrograph and Peak Flow Frequency Analysis
TP-63 HEC Contribution to Reservoir System Operation
TP-64 Determining Peak-Discharge Frequencies in an Urbanizing Watershed: A Case Study
TP-65 Feasibility Analysis in Small Hydropower Planning
TP-66 Reservoir Storage Determination by Computer Simulation of Flood Control and Conservation Systems
TP-67 Hydrologic Land Use Classification Using LANDSAT
TP-68 Interactive Nonstructural Flood-Control Planning
TP-69 Critical Water Surface by Minimum Specific Energy Using the Parabolic Method
TP-70 Corps of Engineers Experience with Automatic Calibration of a Precipitation-Runoff Model

TP-71 Determination of Land Use from Satellite Imagery for Input to Hydrologic Models
TP-72 Application of the Finite Element Method to Vertically Stratified Hydrodynamic Flow and Water Quality
TP-73 Flood Mitigation Planning Using HEC-SAM
TP-74 Hydrographs by Single Linear Reservoir Model
TP-75 HEC Activities in Reservoir Analysis
TP-76 Institutional Support of Water Resource Models
TP-77 Investigation of Soil Conservation Service Urban Hydrology Techniques
TP-78 Potential for Increasing the Output of Existing Hydroelectric Plants
TP-79 Potential Energy and Capacity Gains from Flood Control Storage Reallocation at Existing U. S. Hydropower Reservoirs
TP-80 Use of Non-Sequential Techniques in the Analysis of Power Potential at Storage Projects
TP-81 Data Management Systems for Water Resources Planning
TP-82 The New HEC-1 Flood Hydrograph Package
TP-83 River and Reservoir Systems Water Quality Modeling Capability
TP-84 Generalized Real-Time Flood Control System Model
TP-85 Operation Policy Analysis: Sam Rayburn Reservoir
TP-86 Training the Practitioner: The Hydrologic Engineering Center Program
TP-87 Documentation Needs for Water Resources Models
TP-88 Reservoir System Regulation for Water Quality Control
TP-89 A Software System to Aid in Making Real-Time Water Control Decisions
TP-90 Calibration, Verification and Application of a Two-Dimensional Flow Model
TP-91 HEC Software Development and Support
TP-92 Hydrologic Engineering Center Planning Models
TP-93 Flood Routing Through a Flat, Complex Flood Plain Using a One-Dimensional Unsteady Flow Computer Program
TP-94 Dredged-Material Disposal Management Model
TP-95 Infiltration and Soil Moisture Redistribution in HEC-1
TP-96 The Hydrologic Engineering Center Experience in Nonstructural Planning
TP-97 Prediction of the Effects of a Flood Control Project on a Meandering Stream
TP-98 Evolution in Computer Programs Causes Evolution in Training Needs: The Hydrologic Engineering Center Experience
TP-99 Reservoir System Analysis for Water Quality
TP-100 Probable Maximum Flood Estimation - Eastern United States
TP-101 Use of Computer Program HEC-5 for Water Supply Analysis
TP-102 Role of Calibration in the Application of HEC-6
TP-103 Engineering and Economic Considerations in Formulating
TP-104 Modeling Water Resources Systems for Water Quality
TP-105 Use of a Two-Dimensional Flow Model to Quantify Aquatic Habitat
TP-106 Flood-Runoff Forecasting with HEC-1F
TP-107 Dredged-Material Disposal System Capacity Expansion
TP-108 Role of Small Computers in Two-Dimensional Flow Modeling
TP-109 One-Dimensional Model For Mud Flows
TP-110 Subdivision Froude Number
TP-111 HEC-5Q: System Water Quality Modeling
TP-112 New Developments in HEC Programs for Flood Control
TP-113 Modeling and Managing Water Resource Systems for Water Quality
TP-114 Accuracy of Computed Water Surface Profiles - Executive Summary
TP-115 Application of Spatial-Data Management Techniques in Corps Planning
TP-116 The HEC's Activities in Watershed Modeling
TP-117 HEC-1 and HEC-2 Applications on the MicroComputer
TP-118 Real-Time Snow Simulation Model for the Monongahela River Basin
TP-119 Multi-Purpose, Multi-Reservoir Simulation on a PC
TP-120 Technology Transfer of Corps' Hydrologic Models
TP-121 Development, Calibration and Application of Runoff Forecasting Models for the Allegheny River Basin
TP-122 The Estimation of Rainfall for Flood Forecasting Using Radar and Rain Gage Data
TP-123 Developing and Managing a Comprehensive Reservoir Analysis Model
TP-124 Review of the U.S. Army Corps of Engineering Involvement With Alluvial Fan Flooding Problems
TP-125 An Integrated Software Package for Flood Damage Analysis
TP-126 The Value and Depreciation of Existing Facilities: The Case of Reservoirs
TP-127 Floodplain-Management Plan Enumeration
TP-128 Two-Dimensional Floodplain Modeling
TP-129 Status and New Capabilities of Computer Program HEC-6: "Scour and Deposition in Rivers and Reservoirs"
TP-130 Estimating Sediment Delivery and Yield on Alluvial Fans
TP-131 Hydrologic Aspects of Flood Warning - Preparedness Programs
TP-132 Twenty-five Years of Developing, Distributing, and Supporting Hydrologic Engineering Computer Programs
TP-133 Predicting Deposition Patterns in Small Basins
TP-134 Annual Extreme Lake Elevations by Total Probability Theorem
TP-135 A Muskingum-Cunge Channel Flow Routing Method for Drainage Networks

REPORT DOCUMENTATION PAGE

Form Approved
OMB No. 0704-0188

1a REPORT SECURITY CLASSIFICATION UNCLASSIFIED	1b RESTRICTIVE MARKINGS
2a SECURITY CLASSIFICATION AUTHORITY	3 DISTRIBUTION/AVAILABILITY OF REPORT Distribution of this publication is unlimted
2b DECLASSIFICATION/DOWNGRADING SCHEDULE	
4 PERFORMING ORGANIZATION REPORT NUMBER(S) Technical Paper No. 135	5 MONITORING ORGANIZATION REPORT NUMBER(S)
6a NAME OF PERFORMING ORGANIZATION US Army Corps of Engineers Hydrologic Engineering Center 6b OFFICE SYMBOL (If applicable) CEWRC-HEC	7a NAME OF MONITORING ORGANIZATION
6c ADDRESS (City, State, and ZIP Code) 609 Second Street Davis, California 95616	7b ADDRESS (City, State, and ZIP Code)
8a NAME OF FUNDING/SPONSORING ORGANIZATION 8b OFFICE SYMBOL (If applicable)	9 PROCUREMENT INSTRUMENT IDENTIFICATION NUMBER
8c ADDRESS (City, State, and ZIP Code)	10 SOURCE OF FUNDING NUMBERS PROGRAM ELEMENT NO / PROJECT NO / TASK NO / WORK UNIT ACCESSION NO

11 TITLE (Include Security Classification)
A Muskingum-Cunge Channel Flow Routing Method for Drainage Networks

12 PERSONAL AUTHOR(S)
Jurgen Gorbrecht and Gary W. Brunner

13a TYPE OF REPORT	13b TIME COVERED	14 DATE OF REPORT (Year, Month, Day)	15 PAGE COUNT
Final	FROM _____ TO _____	November 1991	30

16 SUPPLEMENTARY NOTATION
This paper was published in the ASCE Journal of Hydraulics, Volume 117, No. 5, May 1991.

17 COSATI CODES			18 SUBJECT TERMS (Continue on reverse if necessary and identify by block number)
FIELD	GROUP	SUB-GROUP	Muskingum-Cunge, Channel Flow Routing, drainage networks, Compound Cross-Sections, variable time step.

19 ABSTRACT (Continue on reverse if necessary and identify by block number)

A Muskingum-Cunge channel flow routing scheme is modified for application to large drainage networks with compound cross sections and for continuous long-term simulation. The modifications consist of a decoupling and separate routing of main and overbank channel flow, an introduction of a variable time step to increase model efficiency during periods of steady flow, and an interval determination of the numerical increment. The resulting hydrologic model is verfied by comparing its flow routing results with those of hydraulic benchmark models solving the full unsteady flow equations. Test conditions consist of hypothetical flood hydrographs, long prismatic channels with simple and compound sections, and a third order drainage network. For the tested conditions, the model produces hydrograph peaks, times to peak and shapes that compare well with those of the hydraulic benchmarks. Hydrograph distortions due to overbank flood plain storage and multiple peaks from complex drainage networks are also well reproduced. The execution time of the model is generally one order of magnitude faster than that of the hydraulic benchmark models.

20 DISTRIBUTION/AVAILABILITY OF ABSTRACT	21 ABSTRACT SECURITY CLASSIFICATION	
☒ UNCLASSIFIED/UNLIMITED ☐ SAME AS RPT ☐ DTIC USERS	Unclassified	
22a NAME OF RESPONSIBLE INDIVIDUAL Gary W. Brunner	22b TELEPHONE (Include Area Code) 916 756-1104	22c OFFICE SYMBOL CEWRC-HEC-T

DD Form 1473, JUN 86 *Previous editions are obsolete.*